

# ASYMPTOTICS AND MONODROMY OF THE ALGEBRAIC SPECTRUM OF QUASI-EXACTLY SOLVABLE SEXTIC OSCILLATOR

BORIS SHAPIRO AND MILOŠ TATER

**ABSTRACT.** Below we study theoretically and numerically the asymptotics of the algebraic part of the spectrum for the quasi-exactly solvable sextic potential  $\Pi_{m,p,b}(x) = x^6 + 2bx^4 + (b^2 - (4m+3))x^2$ , its level crossing points, and its monodromy in the complex plane of parameter  $b$ . Here  $m$  is a fixed positive integer. We also discuss connection between the quasi-exactly solvable sextic and the classical quartic potential.

## 1. INTRODUCTION

To the best of our knowledge, historically first, and the most well-known example of a quasi-exactly solvable potential in quantum mechanics is the quasi-exactly solvable sextic. It was originally discovered in [16] (see also [17], [18],[20]) and it is given by:

$$\Pi_{m,p,b}(x) = x^6 + 2bx^4 + (b^2 - (4m+2p+3))x^2,$$

where  $m$  is a fixed positive integer,  $p \in \{0, 1\}$ , and  $b$  is an arbitrary complex number. In [18] it was shown that, for any value of  $b$ , the Schrödinger equation

$$T = -\frac{d^2}{dx^2} + \Pi(x) = \lambda y \quad (1.1)$$

with the boundary conditions

$$y(\pm\infty) = 0$$

on  $\mathbb{R}$ , has  $m+1$  eigenfunctions of the form

$$\phi(x) = Q(x)e^{-\frac{x^4}{4} - \frac{bx^2}{2}}, \quad (1.2)$$

where  $Q(x)$  is an even (resp. odd) polynomial of degree  $2m$  (resp.  $2m+1$ ) for  $p=0$  (resp.  $p=1$ ). The above eigenfunctions as well as their eigenvalues can be found by a simple algebraic procedure presented below. The latter eigenvalues form the so-called *algebraic part* of the spectrum of  $T$ . For any real value of parameter  $b$ , these eigenvalues are real and distinct. A number of their properties is discussed in e.g., [1], [2], [17], [19].

Let us briefly recall how, for any value of  $b$ , to describe the algebraic part of the spectrum explicitly. Simple calculation shows that if an eigenfunction  $\phi(x)$  of the form (1.2) has an eigenvalue  $\lambda$ , then its polynomial factor  $Q(x)$  satisfies the differential equation:

$$-Q''(x) + 2(x^3 + bx)Q'(x) - ((4m+2p)x^2 - b)Q(x) = \lambda Q(x). \quad (1.3)$$

The differential operator

$$\mathfrak{d} = -\frac{d^2}{dx^2} + 2(x^3 + bx)\frac{d}{dx} - ((4m+2p)x^2 - b)$$

---

*Date:* August 1, 2018.

*2000 Mathematics Subject Classification.* 81Q10.

*Key words and phrases.* spectrum of an anharmonic oscillator, spectral surface, monodromy.

occurring in the l.h.s. of (1.3) preserves the  $(m+1)$ -dimensional linear space  $V_{ev}$  of all even polynomials of degree  $\leq 2m$  for  $p = 0$ . For  $p = 1$ , it preserves the  $(m+1)$ -dimensional linear space  $V_{odd}$  of all odd polynomials of degree  $\leq 2m+1$ . For  $p = 0$ , using  $t = x^2$ , we can rewrite (1.3) in the form

$$-4t \frac{d^2 Q(t)}{dt^2} + (4t^2 + 4bt - 2) \frac{dQ(t)}{dt} - (4mt - b)Q(t) = \lambda Q(t), \quad (1.4)$$

which is a special case of the double-confluent Heun equation.

Thus, the algebraic part of the spectrum of the Schrödinger operator  $T$  is simply the spectrum of the operator  $\mathfrak{d}$  restricted to  $V_{ev}$  for  $p = 0$  (resp. to  $V_{odd}$  for  $p = 1$ ). Fixing the usual monomial basis  $(1, x^2, x^4, \dots, x^{2m})$  in  $V_{ev}$  and  $(x, x^3, \dots, x^{2m+1})$  in  $V_{odd}$ , we can explicitly calculate the action of  $\mathfrak{d}$  on the respective space.

Below we will concentrate on the case  $p = 0$ . (Case  $p = 1$  is very similar.) Straight-forward calculation shows that, for  $p = 0$ , the  $(m+1) \times (m+1)$ -matrix  $M_m(b)$  representing the action of  $\mathfrak{d}$  in the monomial basis  $(1, t, t^2, \dots, t^m)$  of  $V_{ev}$  coincides with

$$M_m(b) = \begin{pmatrix} b & -4m & 0 & 0 & 0 & \dots \\ -1 \cdot 2 & 5b & 4 - 4m & 0 & 0 & \dots \\ 0 & -3 \cdot 4 & 9b & 8 - 4m & 0 & \dots \\ 0 & 0 & -5 \cdot 6 & 13b & 12 - 4m & \dots \\ \vdots & \vdots & \vdots & \vdots & \vdots & \ddots \end{pmatrix}. \quad (1.5)$$

In what follows, we mainly study different asymptotic spectral properties of  $M_m(b)$ . The structure of the paper is as follows. In § 2 we study the spectral asymptotics of the sequence  $\{M_m(b)\}$  (after appropriate scaling) as well as the properties of the sequence of eigenpolynomials corresponding to a converging sequence of the latter eigenvalues. Observe that most of the arguments presented § 2 are not mathematically rigorous since we are missing proofs of several convergence statements. However our arguments provide a natural and numerically supported heuristics. In § 3 we present our numerical results and conjectures about the level crossing points and the monodromy of the spectrum of  $M_m(b)$ , when  $b$  traverses closed loops in the complex plane avoiding the level crossing points. Based on our guesses we also formulate the explicit conjecture about the monodromy of the classical quartic potential studied in a large number of papers starting with [4].

Observe that our “results” below are similar to that of our previous article [15], where the case of quasi-exactly solvable quartic was considered in some details. Although at present we do not know how one can prove our guesses rigorously, due to their potential importance for physics and many surprising features, we were advised by a number scientists including Professors B. Simon and C. M. Bender to make our “results” available to the mathematics and physics communities.

**Acknowledgements.** The first author wants to thank Professors A. Eremenko and A. Gabrielov of Purdue University for numerous discussions. The first author is grateful to the Nuclear Physics Institute at Řež of the Czech Academy of Sciences for the hospitality in November 2016. The second author acknowledges the hospitality of the Department of Mathematics, Stockholm university in April 2016. His research was supported by the Czech Science Foundation (GACR) within the project 14-06818S.

## 2. SPECTRAL ASYMPTOTICS

To study the characteristic polynomial of the tridiagonal matrix (1.5), we follow the circle of ideas developed in [9] and use the characteristic polynomials of its principle minors. Namely, denote by  $\Delta_m^{(i)}$ ,  $i = 1, \dots, m+1$  the determinant of the

$i$ -th principal minor of  $\lambda I_{m+1} - M_m(b)$ , where  $I_{m+1}$  is the identity matrix of size  $m+1$ . This finite sequence of characteristic polynomials satisfies the recurrence relation

$$\Delta_m^{(i)} = (\lambda - (4i-3)b)\Delta_m^{(i-1)} - 4(2i-2)(2i-3)(m+2-i)\Delta_m^{(i-2)}, \quad i = 1, \dots, m+1 \quad (2.1)$$

with the initial conditions:  $\Delta_m^{(-1)} = 0$  and  $\Delta_m^{(0)} = 1$ . Observe that, for any fixed real  $b$ ,  $\{\Delta_m^{(i)}\}_{i=0}^{m+1}$  is a sequence of discrete orthogonal polynomials.

Denoting by  $D_m(\lambda, b) := \Delta_m^{(m+1)}(\lambda, b)$ , it was proven in [14] that, for any fixed  $b$ , the maximal absolute value of the roots of  $D_m(\lambda, b)$  grows as  $16m^{3/2}/3\sqrt{3}$  and the density of the asymptotic root distribution of the scaled polynomials  $\{D_m(m^{3/2}\tilde{\lambda}, b)\}$  coincides with that of  $\{D_m(m^{3/2}\tilde{\lambda}, 0)\}$  and is given by the integral

$$\frac{C}{\pi} \int_0^1 \frac{d\tau}{\sqrt{64\tau(\tau-1)^2 - C^2x^2}},$$

where  $x \in [-C, C]$  and  $C = 16/3\sqrt{3}$ ; see also [2].

Therefore, if we keep  $b$  fixed and scale  $\lambda$  as above, we get the same standard limiting distribution. Using the corresponding three-term recurrence relation, one can easily guess that an interesting dependence of the sequence of spectra on  $b$  implying stabilisation of the spectral distribution might happen if one takes the sequence of matrices

$$\widetilde{M}_m(b) = \begin{pmatrix} \frac{b}{m} & \frac{-4m}{m^{3/2}} & 0 & 0 & 0 & \dots \\ \frac{-1.2}{m^{3/2}} & \frac{5b}{m} & \frac{4-4m}{m^{3/2}} & 0 & 0 & \dots \\ 0 & \frac{-3.4}{m^{3/2}} & \frac{9b}{m} & \frac{8-4m}{m^{3/2}} & 0 & \dots \\ 0 & 0 & \frac{-5.6}{m^{3/2}} & \frac{13b}{m} & \frac{12-4m}{m^{3/2}} & \dots \\ \vdots & \vdots & \vdots & \vdots & \vdots & \ddots \end{pmatrix}, \quad (2.2)$$

which is equivalent to scaling  $b_m = bm^{1/2}$  and  $\tilde{\lambda} = \lambda/m^{3/2}$  in (1.5). In terms of the original equation (1.4), we study degree  $m$  polynomial solutions of the differential equation

$$-4t \frac{d^2 Q(t)}{dt^2} + (4t^2 + 4bm^{1/2}t - 2) \frac{dQ(t)}{dt} - (4mt - bm^{1/2})Q(t) = \tilde{\lambda}m^{3/2}Q(t). \quad (2.3)$$

The characteristic polynomials  $\tilde{\Delta}_m^{(i)}(\tilde{\lambda}, b)$  of the principal minors of (2.2) satisfy the modified 3-term recurrence

$$\tilde{\Delta}_m^{(i)} = \left( \tilde{\lambda} - \frac{4i-3}{m}b \right) \tilde{\Delta}_m^{(i-1)} - \frac{4(2i-2)(2i-3)(m+2-i)}{m^3} \tilde{\Delta}_m^{(i-2)}, \quad (2.4)$$

where  $\tilde{\Delta}_m^{(-1)} = 0$ ,  $\tilde{\Delta}_m^{(0)} = 1$ . See examples in Fig. 1.

Set  $\tilde{D}_m(\tilde{\lambda}, b) := \tilde{\Delta}_m^{(m+1)}(\tilde{\lambda}, b)$ . Below, for any given  $b$ , we will study the asymptotic root-counting measure  $\mu_b$  of the polynomial sequence  $\{\tilde{D}_m(\tilde{\lambda}, b)\}$ . By the main result of [9], the Cauchy transform of  $\mu_b$  outside a certain bounded domain in  $\mathbb{C}$  can be calculated by averaging the Cauchy transforms of polynomial sequences in a 1-parameter family (depending on parameter  $\tau \in [0, 1]$ ) which is obtained from (2.4) by taking the limit  $\frac{i}{m} \rightarrow \tau$ . In other words, we need to consider the one-parameter family of three-term recurrence relations of the form

$$\Delta_\tau^{(i)} = (\tilde{\lambda} - 4\tau b)\Delta_\tau^{(i-1)} - 4(2\tau)^2(1-\tau)\Delta_\tau^{(i-2)}, \quad \tau \in [0, 1]. \quad (2.5)$$

The characteristic equation of (2.5) is given by

$$\Psi^2 = (\tilde{\lambda} - 4\tau b)\Psi - 16\tau^2(1-\tau).$$

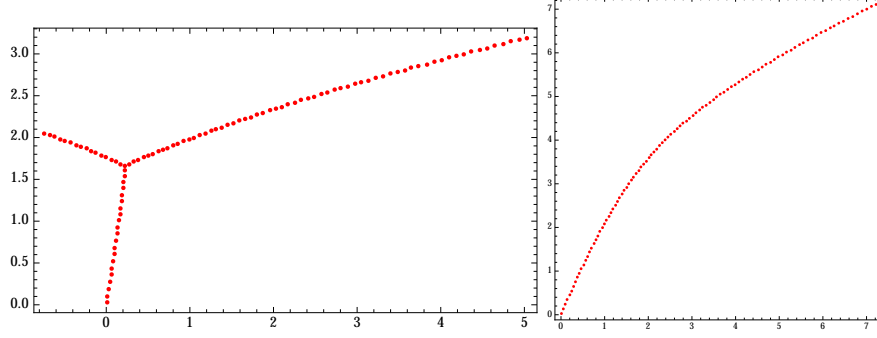


FIGURE 1. The spectra of  $\widetilde{M}_{100}(b)$  for  $b = (3/4 + I)$  (left) and  $b = 3/2 + 2I$  (right).

Its branch points with respect to  $\Psi$  (i.e. the values of  $\tilde{\lambda}$  for which the latter characteristic equation has a double root with respect to  $\Psi$ ) are determined by the relation

$$(\tilde{\lambda} - 4\tau b)^2 = 64\tau^2(1 - \tau).$$

In other words,

$$\tilde{\lambda}_{1,2}(\tau) = 4\tau b \pm 8\sqrt{\tau^2(1 - \tau)}, \quad \tau \in [0, 1]. \quad (2.6)$$

By [9], in the complement of the domain traversed by the family of the straight segments  $[\tilde{\lambda}_1(\tau), \tilde{\lambda}_2(\tau)]$  in  $\mathbb{C}$ , where  $\tau$  runs over the interval  $[0, 1]$ , the Cauchy transform of  $\mu_b$  is given by the integral formula

$$C_b(z) = \int_0^1 \frac{d\tau}{\sqrt{(z - 4\tau b)^2 - 64\tau^2(1 - \tau)}}. \quad (2.7)$$

If  $b$  is real, then each interval  $[\tilde{\lambda}_1(\tau), \tilde{\lambda}_2(\tau)]$  is real and one can show that

$$\bigcup_{\tau \in [0, 1]} [\tilde{\lambda}_1(\tau), \tilde{\lambda}_2(\tau)] = \left[ \frac{2}{27} \left( 36b - b^3 - \sqrt{(12 + b^2)^3} \right), \frac{2}{27} \left( 36b - b^3 + \sqrt{(12 + b^2)^3} \right) \right].$$

The density of  $\mu_b$  on the latter interval can be represented by the integral formula similar to the case  $b = 0$  given above.

If  $b = u + iv$  with  $v \neq 0$ , then the family of the above endpoints (2.6) traverses the oval of the real rational cubic  $\Gamma_b$  with a node at the origin given by the equation

$$\Gamma_b : \left( x - \frac{uy}{v} \right)^2 = \frac{(4v - y)y^2}{v^3}, \quad (2.8)$$

where  $x = \operatorname{Re} z$  and  $y = \operatorname{Im} z$ , see examples in Fig. 2. Explicit parameterisation of  $\Gamma_b$  as a rational curve is given by

$$\begin{cases} x = \frac{2v\nu}{(1-\nu^2)^3} (4(1-\nu^2)^2 - (2v\nu - u(1-\nu^2))^2) \\ y = \frac{v}{(1-\nu^2)^2} (4(1-\nu^2)^2 - (2v\nu - u(1-\nu^2))^2). \end{cases}$$

(To get the oval,  $\nu$  has to run between the roots of the equation  $4(1-\nu^2)^2 - (2v\nu - u(1-\nu^2))^2 = 0$ .)

Recall that the general notion of (real) foci of real algebraic curves was developed by J. Plücker around 1832 and these foci are the intersections with the real plane of the complex tangent lines to the complexification of the original curve passing through the so-called circular points at infinity. In the homogeneous coordinates

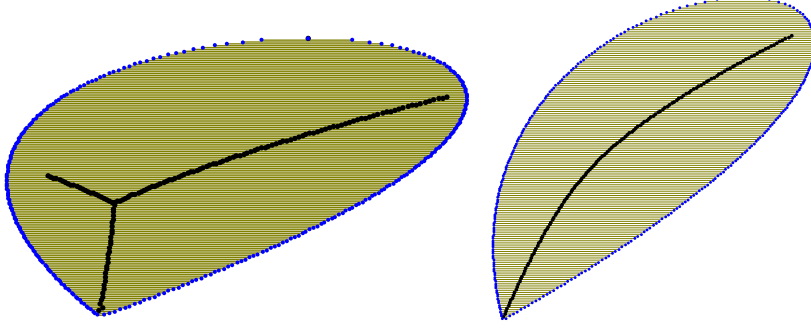


FIGURE 2. The spectra of  $\widetilde{M}_{100}(b)$  for  $b = (3/4 + I)$  (left) and  $b = 3/2 + 2I$  (right) with the corresponding ovals and foci.

$(X, Y, Z)$  of the plane  $(x, y)$ , these circular points are given by  $(1, \pm I, 0)$ , see e.g. [11]. The easiest way to find the foci of a real plane algebraic curve given by the equation  $F(x, y) = 0$  is to substitute  $y = Ix + f$  in  $F$  and to calculate the discriminant of the resulting polynomial with respect to  $x$ . This leads to the polynomial equation in the variable  $f$  whose roots are the foci of the original curve, see e.g. [6]. In the case of the singular cubic  $\Gamma_b$ , we get the equation

$$f^2(27f^2 + 4f(b^3 - 36b) - 16(4 - b^2)^2) = 0. \quad (2.9)$$

Equation (2.9) has a double root at the origin and two more foci  $f_{1,2}$  given by

$$f_{1,2} = \frac{2}{27} \left( 36b - b^3 \pm \sqrt{(12 - b^2)^3} \right).$$

Observe that, in the case of real  $b$ ,  $f_{1,2}$  coincide with the endpoints of the interval  $\bigcup_{\tau \in [0,1]} [\widetilde{\lambda}_1(\tau), \widetilde{\lambda}_2(\tau)]$  obtained above. Our numerical results strongly support the following conjecture.

**Conjecture 1.** *Depending of the value of  $b$ , the endpoints of the support of  $\mu_b$  are either all three foci of  $\Gamma_b$  or just two of them always including the focus at the origin, see Fig. 2.*

In order to characterize the support of  $\mu_b$  completely, we suggest the following heuristic argument. Let  $\widetilde{\lambda}_{j_m, m}$  be an eigenvalue of (2.3). Abusing our notation, denote by  $p_m(t)$  the eigenpolynomial whose eigenvalue equals  $\widetilde{\lambda}_{j_m, m}$ . It satisfies the differential equation

$$-4tp_m'' + (4t^2 + 4bm^{1/2}t - 2)p_m' - (4mt - bm^{1/2} + \widetilde{\lambda}_{j_m, m}m^{3/2})p_m = 0. \quad (2.10)$$

Let us choose a (sub)sequence  $\{\widetilde{\lambda}_{j_m, m}\}_{m=1}^\infty$  of the eigenvalues of  $\widetilde{M}_m(b)$  (one  $j_m$  for each  $m$ ) and assume that it converges to some complex number  $\Lambda$ . In other words,  $\Lambda = \lim_{m \rightarrow \infty} \widetilde{\lambda}_{j_m, m}$ . Let  $\{p_m(t)\}_{m=1}^\infty$  be the sequence of corresponding eigenpolynomials, and  $\{\kappa_m\}_{m=1}^\infty$  be the sequence of their root-counting measures. One can easily observe that the sequence  $\{\kappa_m\}_{m=1}^\infty$  does not converge without appropriate scaling. Scaling the variable  $t$  in the  $m$ -th eigenpolynomial as  $t = \Theta m^{1/2}$ ,  $\Theta$  being the new scaled time variable, we transform equation (2.10) into

$$\frac{-4\Theta}{m^{1/2}} \frac{d^2 p_m}{d\Theta^2} + \frac{(4m\Theta^2 + 4mb\Theta - 2)}{m^{1/2}} \frac{dp_m}{d\Theta} - (4m^{3/2}\Theta - bm^{1/2} + \widetilde{\lambda}_{j_m, m}m^{3/2})p_m = 0.$$

Dividing the above equation by  $m^{3/2}p_m$ , we get

$$-4\Theta \frac{\frac{d^2 p_m}{d\Theta^2}}{m^2 p_m} + \left(4\Theta^2 + 4b\Theta - \frac{2}{m}\right) \frac{\frac{dp_m}{d\Theta}}{mp_m} - \left(4\Theta - \frac{b}{m} + \tilde{\lambda}_{j_m, m}\right) = 0. \quad (2.11)$$

Denote by  $\{\tilde{\kappa}_m\}_{m=1}^\infty$  the sequence of the root-counting measures of the scaled eigenpolynomials  $p_m(m^{1/2}\Theta)$ . Assuming that the weak limit  $\lim_{m \rightarrow \infty} \tilde{\kappa}_m$  exists, denote it by  $\Omega$ . Then,

$$\lim_{m \rightarrow \infty} \frac{\frac{dp_m}{d\Theta}}{mp_m} = \mathcal{C}_\Omega \quad \text{and} \quad \lim_{m \rightarrow \infty} \frac{\frac{d^2 p_m}{d\Theta^2}}{m^2 p_m} = \mathcal{C}_\Omega^2,$$

where the limits are understood as distributions. Thus under the convergence assumption, the Cauchy transform  $\mathcal{C}_\Omega$  of the limiting measure  $\Omega$  satisfies a.e. in  $\mathbb{C}$  the algebraic equation

$$\Theta \mathcal{C}_\Omega^2 - \Theta(\Theta + b)\mathcal{C}_\Omega + (\Theta + \Lambda/4) = 0, \quad (2.12)$$

where  $\Lambda = \lim_{m \rightarrow \infty} \tilde{\lambda}_{j_m, m}$ . The fact that (2.12) admits a solution which is the Cauchy transform of a probability measure supported on a finite number of compact semi-analytic curves and points imposes strong restriction on the possible values of  $\Lambda$ .

We need the following statement, see [3].

**Lemma 1.** *If the Cauchy transform  $\mathcal{C}_\nu$  of a probability measure  $\nu$  satisfies a.e. in  $\mathbb{C}$  a quadratic equation*

$$Q_2(z)\mathcal{C}_\nu^2 + Q_1(z)\mathcal{C}_\nu + Q_0(z) = 0,$$

*then the support of  $\nu$  consists of finitely many semi-analytic curves which are horizontal trajectories of the quadratic differential  $\Psi = -\frac{Q_1^2 - 4Q_2Q_0}{Q_2^2}dz^2$ . In particular, the finite endpoints of the support are either the roots of  $Q_1^2 - 4Q_2Q_0$  or the roots of  $Q_2$ .*

In our case the corresponding quadratic differential is

$$\Psi_{b, \Lambda} = -\frac{\Theta(\Theta + b)^2 - 4\Theta - \Lambda}{\Theta} d\Theta^2. \quad (2.13)$$

**Lemma 2.** *The set of critical  $\Lambda$  of the polynomial  $P(\Theta) = \Theta(\Theta + b)^2 - 4\Theta - \Lambda$ , (i.e., the set of  $\Lambda$  for which  $P(\Theta)$  has a double root w.r.t  $\Theta$ ) coincides with the foci (2.9).*

*Proof.* Straight-forward calculation.  $\square$

For generic  $\Lambda$ , the differential  $\Psi_{b, \Lambda}$  has three simple zeros and one simple pole at 0. Since  $\Omega$  has bounded support and the Cauchy transform  $\mathcal{C}_\Omega$  is univalent in the complement to the support of  $\Omega$  (which consists of a finite number of compact curves and points), then  $\Psi_{b, \Lambda}$  must have two critical trajectories one of which connects two (simple) zeros and the other connects the pole at the origin and the remaining zero. This reasoning motivates the following claim.

**Conjecture 2.** *The support of  $\mu_b$  coincides with the set of values of  $\Lambda$  such that the differential (2.13) has two critical horizontal trajectories.*

### 3. NUMERICAL RESULTS ON THE LEVEL CROSSING POINTS AND SPECTRAL MONODROMY OF QES-SEXTIC

**3.1. Level crossing points.** For any fixed  $b$ , the spectrum of  $M_m(b)$  is the zero locus of the bivariate polynomial  $D_m(\lambda, b)$  with respect for the variable  $\lambda$ . For a generic value of  $b$ , the spectrum of  $M_m(b)$  consists of  $m + 1$  distinct points. By definition, the level crossing  $\Sigma_m \subset \mathbb{C}$  of  $M_m(b)$  is the set of all values of  $b$ , for which the spectrum of  $M_m(b)$  contains less than  $m + 1$  distinct points.  $\Sigma_m$  is the zero locus of the discriminant  $\mathcal{D}_m(b)$  of  $D_m(\lambda, b)$  determined as

$$\mathcal{D}_m(b) := \text{Resultant} \left( D_m(\lambda, b), \frac{\partial D_m(\lambda, b)}{\partial \lambda}, \lambda \right).$$

One can easily check that  $\deg \mathcal{D}_m(b) = m(m + 1)$ . Observe that  $\mathcal{D}_m(b)$  is a real univariate polynomial without real roots. Thus the set  $\Sigma_m$  consists of  $\binom{m+1}{2}$  (not necessarily distinct) complex conjugate pairs of points. The level crossing sets  $\Sigma_{10}(b)$  and  $\Sigma_{20}(b)$  are shown in Fig. 3. (Similar picture can be found in [8].) Our experiments in Mathematica for  $m \leq 25$  show that:

- (i)  $\Sigma_m$  forms a lattice-like pattern whose outer boundary is a curvilinear rombus. The level crossing points in the upper and lower half planes are naturally organized in “horizontal” rows with  $m, m - 1, \dots, 1$  points respectively, see Fig. 3.
- (ii) the sizes of the rhombi grow as  $\sqrt{12m}$ , see Fig. 4;
- (iii) after scaling by  $\sqrt{m}$ , the sequence of root counting measures of  $\Sigma_m$  converges to a continuous measure  $\mu_b$  supported on the curvilinear rhombus  $\mathfrak{R} \subset \mathbb{C}$  in the complex  $b$ -plane such that if  $b \in \mathfrak{R}$ , then the support of  $\mu_b$  consists of three legs ending at 0 and both foci  $f_1, f_2$ , see Fig.2 left. If  $b \in \mathbb{C} \setminus \mathfrak{R}$ , then the support of  $\mu_b$  consists of one leg ending at 0 and one of the foci  $f_1, f_2$ , see Fig.2 right. The boundary of  $\mathfrak{R}$  consists of those  $b$  for which one focus lies on the leg connecting 0 with the other focus, see Fig. 5. Conjecturally, the four vertices of  $\mathfrak{R}$  are  $\pm 2$  and  $\pm\sqrt{12}I$ . At  $b = \pm 2$  one of the foci coincides with 0 and at  $b = \pm\sqrt{12}I$  the foci coincide with each other.
- (iii) after appropriate rescaling, the distribution of level crossings near the center of each of curvilinear triangles converge to a regular hexagonal lattice, see Fig. 6. (Close to the center of the curvilinear triangle in Fig. 6 the picture resembles a hexagonal lattice.)

**3.2. Monodromy.** Below, based on our numerical results obtained for  $m \leq 10$ , we present, for any positive integer  $m$ , an explicit conjecture completely describing the monodromy of the spectrum of  $M_m(b)$ . Fig. 7 shows these numerical results for  $m = 5$ .

To determine the monodromy operators of the spectrum of  $M_m(b)$ , one needs to choose a system of (based) loops in  $\mathbb{C} \setminus \Sigma_m$  such that they generate the fundamental group of the latter space. Since  $\mathbb{C} \setminus \Sigma_m$  is a wedge of  $m(m + 1)$  circles, we need to choose  $m(m + 1)$  loops in our system. Due to the fact that the spectrum of  $M_m(b)$  is real and simple for all real  $b$  and that  $\Sigma_m$  consists of complex-conjugate pairs, we suggest the following system of loops. For each level crossing point  $b_j = u_j + Iv_j$  in the upper half plane, construct the loop  $\gamma_j$  which starts at  $u_j \in \mathbb{R}$ ; goes up almost to  $b_j$ ; traverses counter-clockwise a small circle centered at  $b_j$ , and returns back to  $u_j$  moving vertically down. Observe that, in principle, such loops can pass through other level crossing points which is forbidden by definition. But our numerical experiments show that:

- (a) such a situation happens only when  $u_j = 0$ , i.e. for the purely imaginary level crossing points, and

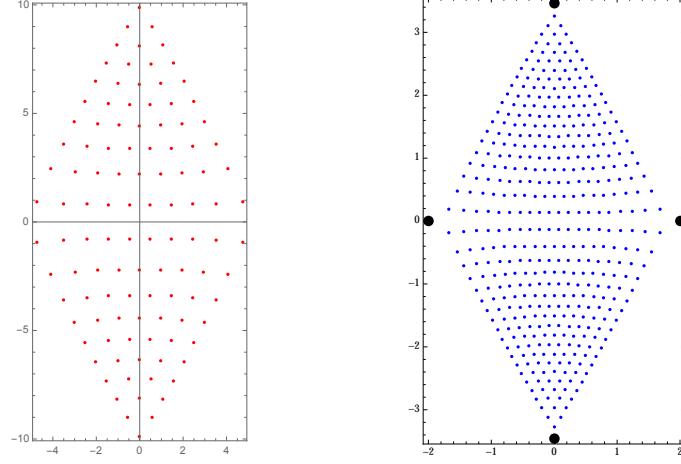


FIGURE 3. Rombi of the level crossing points of the QES-sextic for  $m = 10$  and  $m = 20$  with scaling.

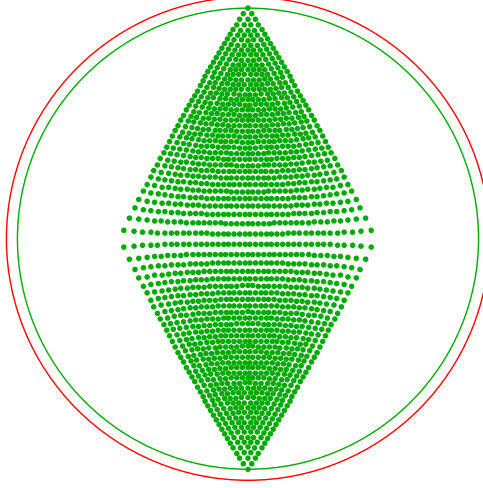


FIGURE 4. Rombi of the level crossing points of the QES-sextic for  $m = 41$ . The red circle has radius  $\sqrt{12 \cdot 41}$ .

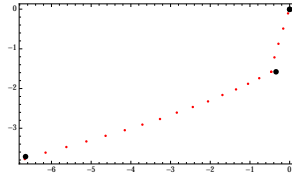


FIGURE 5. The support of  $\mu_b$  for  $b$  on boundary of  $\mathfrak{R}$ .

(b) for the purely imaginary level crossing points, one can make an arbitrary small deformation of  $\gamma_j$  to avoid collision with other crossing points and the resulting monodromy will be independent of the deformation.



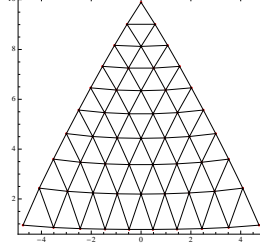


FIGURE 6. Level crossings in the upper half plane for  $m = 10$  with nearest neighbours connected.

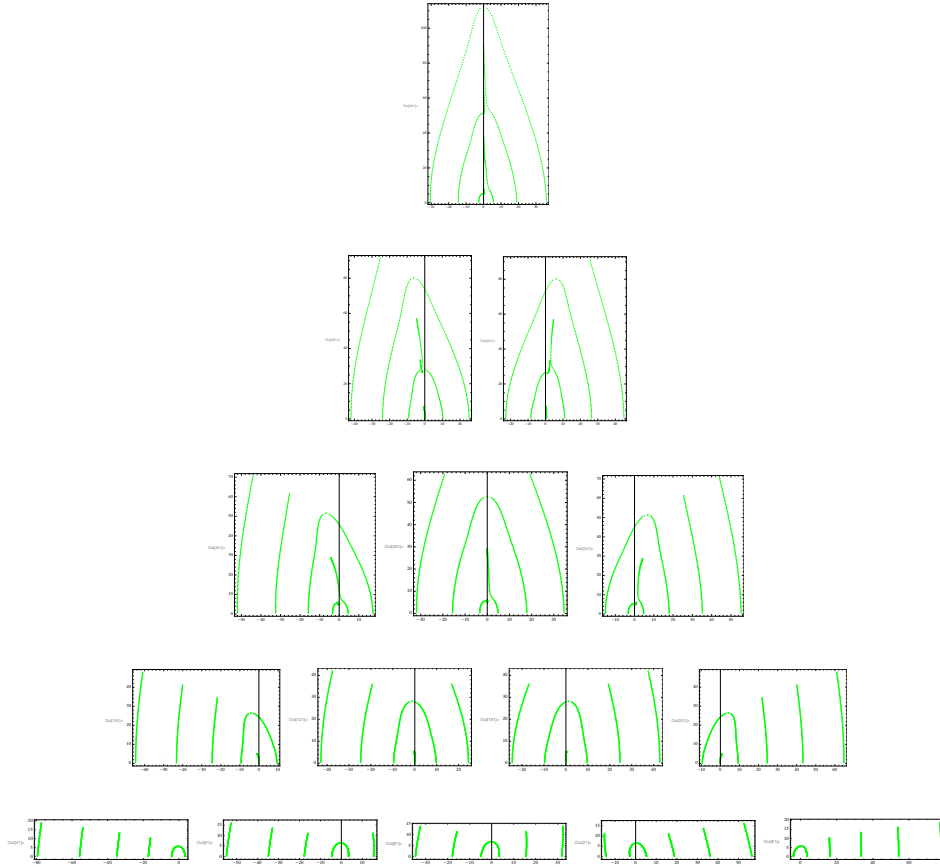


FIGURE 7. Monodromy for  $m = 5$ .

**3.2.1. Monodromy of the algebraic spectrum of QES-sextic oscillator.** By part (i) of the above conjecture about the structure of  $\Sigma_m$ , its level crossings points in the upper half plane are organized in  $m$  “horizontal” rows, where the first row (i.e. the one closest to the real axis) contains  $m$  points, the second row contains  $m - 1$  points,  $\dots$ , the  $m$ -th row contains one point, see Fig. 3.

If we order the level crossing points in the first row from left to right, i.e. according to increase of their real parts, then the corresponding monodromy operators look as follows. If we denote the left-most level crossing point in the first row by

$b_1 = u_1 + iv_1$ , then the permutation of the spectrum of  $M_m(u_1)$  (which consists of  $m+1$  real and distinct points) obtained, when  $b$  traverses the loop  $\gamma_1$ , is the simple transposition  $(m, m+1)$ . In other words, two rightmost points of the spectrum of  $M_m(u_1)$  will change places when  $b$  traverses  $\gamma_1$ . The permutation corresponding to the second level crossing point in the first row is the simple transposition  $(m-1, m)$ . The permutation corresponding to the third level crossing point in the first row is the simple transposition  $(m-2, m-1)$  etc. The case,  $m = 5$  is shown in the last row of Fig. 7.

Similarly, if we order level crossing points in the second row from left to right, i.e., according to increase of their real parts, then the corresponding monodromy operators look as follows. The permutation corresponding to the left-most level crossing point in the second row is the transposition  $(m-1, m+1)$ . The permutation corresponding to the second level crossing point in the second row is the simple transposition  $(m-2, m)$ . The permutation corresponding to the third level crossing point in the first row is the simple transposition  $(m-3, m-1)$  etc. The case,  $m = 5$  is shown in the fourth row of Fig. 7. In the third row we transpose pairs of eigenvalues separated by two intermediate eigenvalues etc. Finally, the transposition corresponding to the only level crossing point on the top is  $(1, m+1)$ , see the first row of Fig. 7.

In other words, level crossing points of  $M_m(b)$  in the upper half plane are in 1-1-correspondence with all transpositions in the symmetric group on  $m+1$  elements; those in the first row corresponding to simple transpositions, those in the second row corresponding to transpositions of pairs of elements which are separated by one intermediate element etc.

*Remark 1.* Pictures in Fig. 7 show the trajectories of the eigenvalues of  $M_m(b)$ , when  $b$  runs vertically from  $u_j \in \mathbb{R}$  to  $b_j = u_j + iv_j$ ,  $b_j$  being some level crossing point. When  $b = u_j$  all the eigenvalues of  $M_m(b)$  are real. When  $b$  moves vertically up, the eigenvalues also move in the complex plane, and when  $b$  reaches  $b_j$  some of the eigenvalues collide. One can trace back which initial eigenvalues collided and knowing that obtain the respective monodromy permutation.

**3.3. QES-sextic and quartic potential.** This material is borrowed from an unpublished preprint [8]. We will present a rescaling of the sequence of QES sextics which converges to the classical quartic oscillator. Recall that the latter oscillator corresponds to the Schrödinger equation

$$-y''(z) + (2z^4 + \beta z^2)y = \mu y \quad (3.1)$$

with the initial conditions  $y(\pm\infty) = 0$  on the real axis.

The spectrum of the classical quartic oscillator was studied in numerous papers since the early days of quantum mechanics, see especially [4, 12, 7, 13, 21] and references therein.

To approximate the quartic potential by a sequence of QES-sextic potentials, set  $n = 4m + 3$ . Then the quasi-exactly solvable equation (1.1) is related to

$$-y''(z) + [a^2 z^6 + 2a\alpha z^4 + (\alpha^2 - an)z^2]y(z) = \mu y(z) \quad (3.2)$$

by the scaling  $x = a^{1/4}z$ ,  $\alpha = a^{1/2}b$ ,  $\lambda = a^{1/2}\mu$ . To approximate the quartic potential  $2z^4 + \beta z^2$  by the rescaled quasi-exactly solvable sextic potentials in (3.2) as  $m \rightarrow \infty$ , let  $\alpha = n^{1/3}(1 + sn^{-2/3})$ ,  $a = n^{-1/3}(1 + tn^{-2/3})$ . Then  $b = \alpha/a^{1/2} = n^{1/2}(1 + (s-t/2)n^{-2/3} + O(n^{-4/3}))$ . Substituting expression for  $a$  and  $\alpha$  into (3.2), we get the potential

$$n^{-2/3}(1 + O(n^{-2/3}))z^6 + 2(1 + (s+t)n^{-2/3} + stn^{-4/3})z^4 + ((2s-t) + s^2n^{-2/3})z^2.$$

Hence  $\beta = 2s - t = 2(n^{-1/2}b - 1)n^{2/3} + O(n^{-2/3})$ .

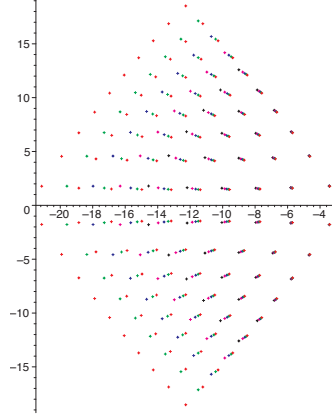
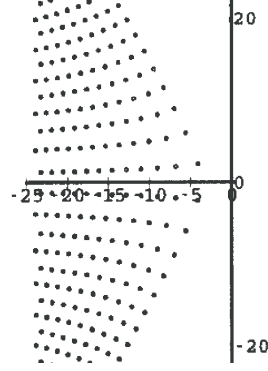
FIGURE 8. Level crossing points for rescaled QES sextics with  $m = 6, 7, 8, 9, 10$ .

FIGURE 9. Level crossing points of the quartic oscillator, see [5].

Figure 8 shows location of the level crossing points of  $\lambda(b)$  for the rescaled sextic, and Figure 9, which is taken from [5] shows the same for the quartic oscillator. (See also Fig. 1 in [13].)

**3.3.1. Monodromy of the full spectrum of the quartic oscillator.** The level crossing set of the quartic oscillator naturally splits into “horizontal” rows, see Fig. 9. Let us order level crossing points in each “horizontal” row from right to left, i.e., in the order of decrease of their real parts. To each level crossing point in the upper half plane of Fig. 9, we associate a loop similar to  $\gamma_j$ ’s above. Namely, we start from the point on the real axis with the same real part as the level crossing point under consideration, move straight up almost reaching the level crossing point, traverse a complete circle around it counterclockwise and go vertically down to the starting point on the real axis. If we now denote by  $b_{k,l} = u_{k,l} + iv_{k,l}$  the  $k$ -th level crossing point in the  $l$ -th “horizontal” row, then the monodromy operator acting on the spectrum of (3.1) with  $\beta = u_{k,l}$  is given by the transposition  $(k, k + l)$ . Here the latter spectrum is real, simple, countable and bounded from below. Its points are naturally labelled by positive integers in the order of increase.

One can find a previous numerical study of the set of level points of the quartic oscillator and an attempt to determine its monodromy in [13].

## 4. FINAL REMARKS

**Problem 1.** Find the linear differential operator of the minimal order such that the latter  $\mathcal{C}_b(z)$  is its solution. (The existence of such an operator is guaranteed by the fact that  $\mathcal{C}_b(z)$  is a Nilsson-class function, [10].)

## REFERENCES

- [1] C. Bender, G. Dunne, Quasi-exactly solvable systems and orthogonal polynomials. J. Math. Phys. 37, (1996), 6–11.
- [2] C. Bender, G. Dunne, M. Moshe, Semiclassical analysis of quasi-exact solvability. Phys. Rev A 55(2), (1997), 2625–2629.
- [3] R. Bøgvad, B. Shapiro, On mother body measures with algebraic Cauchy transform, L'Enseignement Math., to appear.
- [4] C. Bender, T. Wu, Anharmonic oscillator. Phys. Rev. (2) 184, (1969), 1231–1260.
- [5] E. Delabaere, F. Pham, Resurgent methods in semi-classical asymptotics, Annales de l'Inst. Poincaré, sect. A, t. 71 (1999) 1–94.
- [6] A. Emch, On plane algebraic curves with a given system of foci, Bull. AMS, vol 25 (1918), 157–161.
- [7] A. Eremenko and A. Gabrielov, Analytic continuation of eigenfunctions of a quartic oscillator, Comm. math. phys., 287 (2009) 431–457.
- [8] A. Eremenko, A. Gabrielov, Irreducibility of some spectral determinants, arXiv: 0904.1714.
- [9] A. B. J. Kuijlaars, W. Van Assche, *The asymptotic zero distribution of orthogonal polynomials with varying recurrence coefficients*, J. Approx. Theory **99** (1999), 167–197.
- [10] N. Nilsson, *Some growth and ramification properties of certain integrals on algebraic manifold.*, Ark. Mat. 5 1965 463–476 (1965).
- [11] G. Salmon, A treatise on Higher Plane Curves. Intended as a Sequel to a Treatise on Conic Sections, Hodges and Smith, Third Edition, 1879.
- [12] B. Simon, Coupling Constant Analyticity for the Anharmonic Oscillator, Ann. Phys., vol. 58 (1970), 76–136.
- [13] P. Shanley, Spectral properties of the scaled quartic anharmonic oscillator, Ann. Phys. 186 (1988), 292–324.
- [14] B. Shapiro, and M. Tater, Asymptotics of spectral polynomials, Acta Polytechnica vol 47(2-3) (2007) 32–35.
- [15] B. Shapiro, M. Tater, On spectral asymptotics of quasi-exactly solvable quartic and Yablonskii-Vorob'ev polynomials, arXiv:1412.3026, submitted.
- [16] V. Singh, S.N. Biswas and K. Datta, Anharmonic oscillator and the analytic theory of continued fractions, Phys. Rev. D18(1978), 1901–1908.
- [17] A. Turbiner, Quasi-exactly solvable problems and  $\mathfrak{sl}(2)$  algebra, Comm. Math. Phys. 118 (1988). 467–474.
- [18] A. Turbiner, A. Ushveridze, Spectral singularities and the quasi exactly solvable problem, Phys. Lett. 126 A (1987), 181–183.
- [19] A. Ushveridze, Quasi-exactly solvable models in quantum mechanics, Sov. J. Part.Nucl. 20 (1989). 504–528.
- [20] A. Ushveridze, *Quasi-exactly solvable models in quantum mechanics*. Institute of Physics Publishing, Bristol, 1994. xiv+465 pp.
- [21] A. Voros, The return of the quartic oscillator: the complex WKB method. Ann. Inst. H. Poincaré Sect. A (N.S.) 39 (1983), no. 3, 211–338.

DEPARTMENT OF MATHEMATICS, STOCKHOLM UNIVERSITY, SE-106 91 STOCKHOLM, SWEDEN  
*E-mail address:* `shapiro@math.su.se`

DEPARTMENT OF THEORETICAL PHYSICS, NUCLEAR PHYSICS INSTITUTE, ACADEMY OF SCIENCES, 250 68 ŘEŽ NEAR PRAGUE, CZECH REPUBLIC  
*E-mail address:* `tater@ujf.cas.cz`